Electrical crosstalk-coupling measurement and analysis for digital closed loop fibre optic gyro*

Jin Jing(金 靖)†, Tian Hai-Ting(田海亭), Pan Xiong(潘 雄), and Song Ning-Fang(宋凝芳)

School of Instrument Science and Optic-electronics Engineering, Beijing University of Aeronautics and Astronautics, Beijing 100191, *China*

(Received 7 May 2009; revised manuscript received 4 August 2009)

The phase modulation and the closed-loop controller can generate electrical crosstalk-coupling in digital closed-loop fibre optic gyro. Four electrical cross-coupling paths are verified by the open-loop testing approach. It is found the variation of ramp amplitude will lead to the alternation of gyro bias. The amplitude and the phase parameters of the electrical crosstalk signal are measured by lock-in amplifier, and the variation of gyro bias is confirmed to be caused by the alternation of phase according to the amplitude of the ramp. A digital closed-loop fibre optic gyro electrical crosstalk-coupling model is built by approximating the electrical cross-coupling paths as a proportion and integration segment. The results of simulation and experiment show that the modulation signal electrical crosstalk-coupling can cause the dead zone of the gyro when a small angular velocity is inputted, and it could also lead to a periodic vibration of the bias error of the gyro when a large angular velocity is inputted.

Keywords: fibre optic gyro, electrical crosstalk-coupling, open loop testing, correlation detection
PACC: 0760, 0710Y, 0750, 4280

1. Introduction

Two technologies are crucial to the digital closed loop fibre optic gyro (DCL-FOG), namely signal modulation and closed-loop feedback control. Signal modulation is important for improving the accuracy and the anti-interference performance of DCL-FOG; closed-loop feedback control is functional in dynamic range extension and scale factor linearity amelioration of DCL-FOG.[1,2] However, these two technologies are far from flawless. Electrical crosstalk-coupling (ECC) of modulation signal could even lead to bias, dead-zone and periodic vibration of DCL-FOG.[3,4]

Research on the ECC of the modulation signal is currently concentrating on inhibiting method and experimental verification. However, it has neither scrutinised the principle of ECC propagation nor analysed the effect of ECC on DCL-FOG. As proposed in Refs. [1], [3] and [4], the ECC between the phase modulation signal and detector output signal would cause a dead-zone. In Ref. [3], the dead-zone generation condition in specialized modulation was pointed out, and a dead-zone elimination algorithm, which was named as periodic phase bias compensation, was described. The dead-zone phenomena proposed in Refs. [1] and [3] were verified experimentally in Ref. [5]. An ECC elimination algorithm, which is based on correlation and random modulation, is proposed in Refs. [4] and [6].

By open loop testing, four ECC paths are verified to exist in DCL-FOG, and the ECC induced variation of open loop bias, which is related to ramp amplitude, is confirmed to be induced by the variation of difference in the phase between demodulation signal and crosstalk signal. By the model analysis and the measurement, it is verified that this open loop bias causes the dead-zone and the periodic vibration in DCL-FOG as well.

2. Modulation signal crosstalk measurements and analysis

Based on the fundamental principle of DCL-FOG modulation and demodulation,[1] the modulation signal is a combination of analog square wave and ramp wave and the demodulation signal is digital square wave, which should have the same frequency as that of the modulation wave. A bias error would be generated in DCL-FOG if some harmonic wave of the modulation square wave conducts a crosstalk coupling in the front circuit, which is located before the demodulator.

*Project supported by the National High Technology Research and Development Program of China (Grant No. 2007AA04Z436).
†Corresponding author. E-mail: jinjing@buaa.edu.cn
© 2010 Chinese Physical Society and IOP Publishing Ltd

Signal $S_c(t)$ is expressed as the crosstalk signal caused by the coupling of modulation square in the front circuit before the demodulator, and $S_d(t)$ is also expressed as the demodulation square. They are shown as follows:

$$S_c(t) = A_c \cos[(2n-1)(\omega t + \theta_c)], \quad (1)$$

$$S_d(t) = \frac{4}{\pi} \sum_{m=1}^{\infty} \frac{(-1)^{m-1}}{2m-1} \cos[(2m-1)(\omega t + \theta_d)]. \quad (2)$$

After the demodulation and an adequate long period integration, the ECC caused bias in DCL-FOG output is expressed as[1,7]

$$E_{dc} = S_d * S_c = \frac{2A_c(-1)^{n-1}}{\pi(2n-1)} \cos[(2n-1)(\theta_d - \theta_c)], \quad (3)$$

where A_c is the amplitude of crosstalk signal, ω is the basic frequency of modulation square wave, θ_c is the initial phase of crosstalk signal, and θ_d is the initial phase of demodulation square wave.

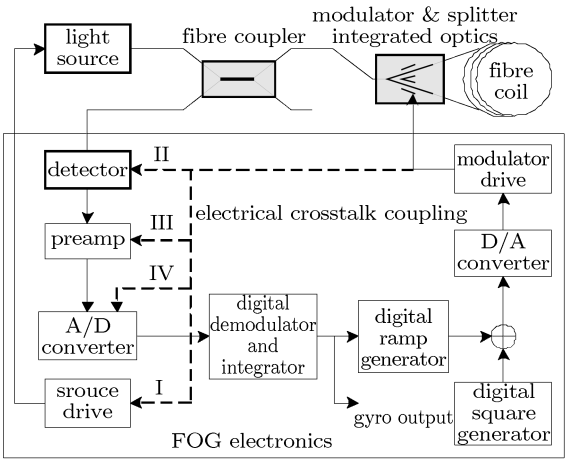


Fig. 1. Typical structure of DCL-FOG and ECC paths.

The typical structure of DCL-FOG is shown in Fig. 1.[1,2,4,8,9] Since the modulator driver and the modulation signal could hardly be segregated physically in circuit design, the modulation crosstalk is inevitable. As shown by dash lines in Fig. 1, the possible ECC paths have four types:

I: the electrical cross-coupling path from the modulator driver to the source driver;

II: the electrical cross-coupling path from the modulator driver to the detector;

III: the electrical cross-coupling path from the modulator driver to the preamp;

IV: the electrical cross-coupling path from the modulator driver to the A/D converter.

The effects of four ECC paths on the FOG output bias are verified via an open loop testing, and the configuration of the testing system is shown in Fig. 1. The light source drive current was set to be 100 mA, and the light power arriving at the detector was about 300 μW. A ramp wave, which was a combination of square wave and fixed step wave was used as a modulation wave. The modulator driver and the modulator were isolated. The amplitude of square wave was 2 V, the frequency was 200 kHz, the amplitude of ramp was 8 V, the period was 580 s and the output integration time was 1 s. The test scheme is listed in Table 1, and the test results are shown in Figs. 2 and 3. In the case where the modulation signal is the square wave only, the results in Fig. 2 show that the bias error caused by the ECC path I is 4.15 °/h, the bias error caused by ECC path II is 3.9 °/h, the bias error caused by ECC path III is 0.55 °/h and the bias error caused by ECC path IV is 0.25 °/h. In the case where the modulation signal is the ramp signal composed of square wave and fixed step wave, the bias error caused by modulation signal crosstalk coupling is a value varying with the amplitude of ramp, the results in Fig. 3 show that the bias error variation caused by ECC path I is 3.49 °/h, the bias error variation caused by ECC path II is 1.2 °/h, the bias error variation caused by ECC path III is 0.4 °/h and the bias error caused by ECC path IV is not observable.

Table 1. Modulation signal ECC test scheme.

modulation wave	connection type of FOG electronic component	included ECC path	bias error curve
square wave	modulator driver and modulator disconnected	I II III IV	*A*
	light source and source driver disconnected	II III IV	*B*
	detector and preamp disconnected	III IV	*C*
	preamp and A/D converter disconnected	IV	*D*
square wave and ramp wave	modulator driver and modulator disconnected	I II III IV	*E*
	light source and source driver disconnected	II III IV	*F*
	detector and preamp disconnected	III IV	*G*
	preamp and A/D converter disconnected	IV	*H*

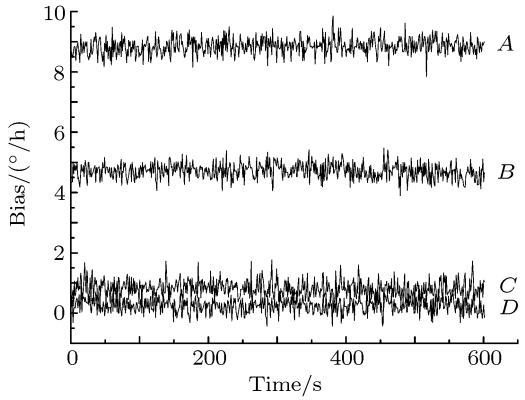


Fig. 2. Open loop bias testing graph generated by electrical cross-coupling under square modulation.

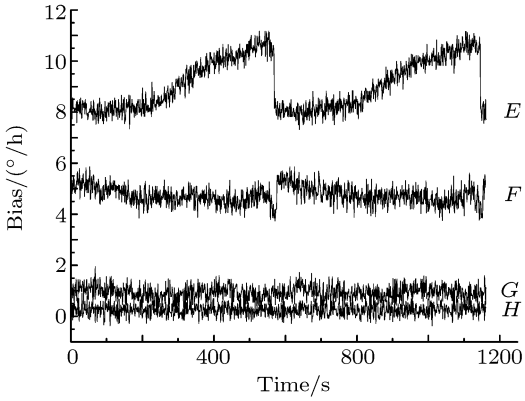


Fig. 3. Open loop bias testing graph generated by electrical cross-coupling under square and ramp combined modulation.

The crosstalk signal from modulation square wave was a periodic signal with the same frequency as that of the modulation square wave. Known from polynomial (3), the modulation signal ECC related to bias $E_{\rm dc}$ is determined by the amplitude $A_{\rm c}$ of crosstalk signal and the difference in phase between demodulation signal and crosstalk signal, $\theta_{\rm d}-\theta_{\rm c}$. Hence, the variation of bias error with ramp amplitude is also determined by the variation of parameter $A_{\rm c}$ or $\theta_{\rm d}-\theta_{\rm c}$ with the ramp amplitude.

The variation of parameters $A_{\rm c}$ and $\theta_{\rm d}-\theta_{\rm c}$ with ramp amplitude was measured by a lock-in amplifier, and the output bias error of FOG was detected via the open loop testing simultaneously. Two probes of the lock-in amplifier were connected with the output terminal of square wave and the analog input terminal of A/D converter separately. For the circuit connection of FOG, the modulator diver and the modulator were disconnected. The parameters of source driver, square wave and the ramp wave were set as before. The testing scenario is shown in Fig. 4, and the testing results are shown in Fig. 5. The amplitude of ramp wave was varied by 8 V, and the amplitude $A_{\rm c}$ of crosstalk signal was 37.65 μV, which could hardly be found to have any change with the variation of ramp wave amplitude. Meanwhile, the difference in phase between demodulation signal and crosstalk signal, $\theta_{\rm d}-\theta_{\rm c}$, varied from 84.7° to 91.5°; The variation of bias error is 3.49°/h. These results show that the variation of bias error with ramp wave amplitude is caused by the variation of parameter $\theta_{\rm d}-\theta_{\rm c}$ with ramp wave amplitude.

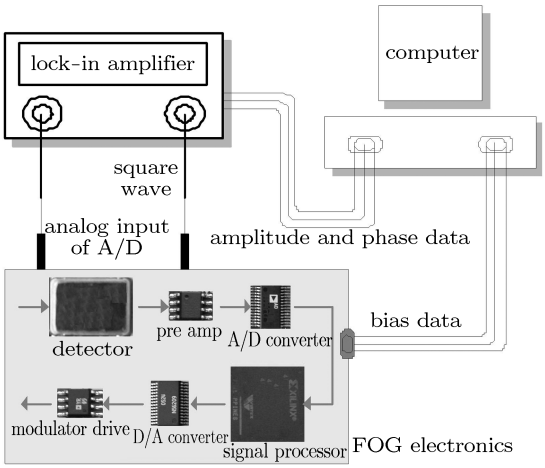


Fig. 4. Testing scenario of crosstalk parameters.

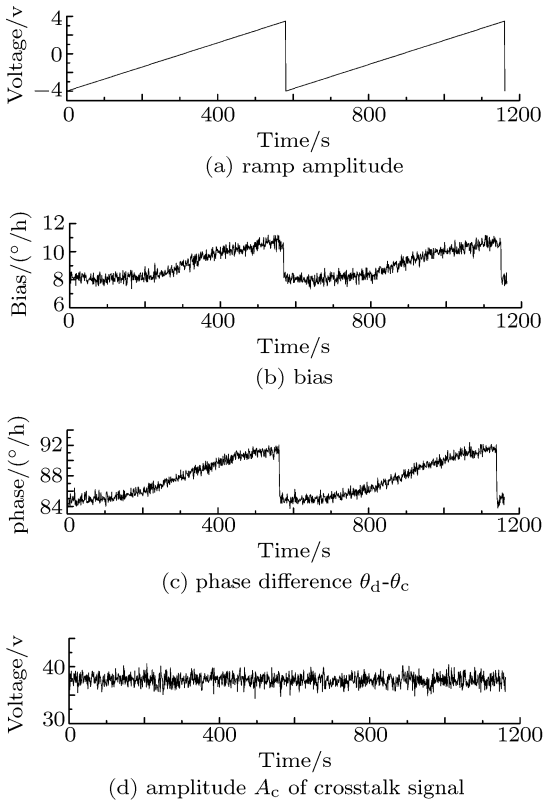


Fig. 5. Testing results of crosstalk parameters.

The variations of $\theta_{\rm d}-\theta_{\rm c}$, $A_{\rm c}$ and bias error at different temperatures were also measured in the same way, the relevant results are listed in Table 2. The results follow that ECC paths and the crosstalk coupling are unstable and vulnerable by ambience.

Table 2. Crosstalk couplings at different temperatures.

temperature /°C	variationof $\theta_{\rm d}-\theta_{\rm c}/(^\circ)$	$A_{\rm c}/\mu$V	variation of bias /(°/h)
–40	13.8	40.59	5.12
25	6.8	37.65	3.49
60	3.4	35.13	1.84

3. Effect of ECC on DCL-FOG

As demonstrated by testing results in the previous section, the difference in phase between modulation signal and crosstalk signal, $\theta_{\rm d}-\theta_{\rm c}$, was located near the 90 ° point. From polynomial (3), it follows that there exists a linear relationship between bias error$E_{\rm dc}$ and phase difference $\theta_{\rm d}-\theta_{\rm c}$, and the correlation factor of $\theta_{\rm d}-\theta_{\rm c}$ and amplitude of ramp wave was 0.9, which is also close to the linear relationship.[10] A simplified DCL-FOG phase model is shown in Fig. 6,[8,11] in which the relationship between ramp wave amplitude and ECC caused bias error is presented approximately as a linear relationship. So, the modulation signal ECC path could be equivalent to a partial integration component and a gain component, which is shown as the dash line in Fig. 6. Only a typical ECC path is imported for the convenience of analysis, which is the ECC path from modulator driver to detector, and the effects of other ECC paths on DCL-FOG are the same as that of this path.

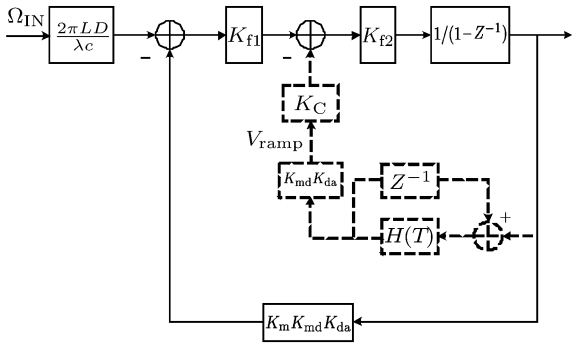


Fig. 6. ECC model of DCL-FOG.

From Fig. 6, it follows that the input–output model equation and the modulated ramp wave voltage equation may be given as follows:

$$\Omega_{\rm o}=\frac{\Omega_{\rm IN}K_0K_{\rm f1}K_{\rm f2}-V_{\rm ramp}K_{\rm c}K_{\rm f2}}{K_{\rm m}K_{\rm md}K_{\rm da}K_{\rm f1}K_{\rm f2}+(1-Z^{-1})}, \tag{4}$$

$$V_{\rm ramp}=\frac{\Omega_{\rm IN}K_0K_{\rm f1}K_{\rm f2}K_{\rm md}K_{\rm da}H(T)}{K_{\rm m}K_{\rm md}K_{\rm da}K_{\rm f1}K_{\rm f2}[1-H(T)Z^{-1}]+H(T)K_{\rm md}K_{\rm da}K_{\rm c}K_{\rm f2}+(1-Z^{-1})[1-H(T)Z^{-1}]}, \tag{5}$$

where $K_0=2\pi ld/\lambda c$, $\Omega_{\rm IN}$ is the input angular velocity, $\Omega_{\rm o}$ is the output angular velocity, l is the length of fibre, d is the diameter of fibre coil, λ is the wavelength of light and c is the light speed in vacuum. Parameter $K_{\rm f1}$ is related to source output power, optical loss and detector responsivity, $K_{\rm f2}$ is dependent on preamp gain factor, A/D converter gain factor and demodulation gain factor, $K_{\rm m}$ is the modulator efficiency, $K_{\rm da}$ is the D/A converter gain factor, $K_{\rm md}$ is the modulator driver gain factor, and $K_{\rm c}$ is the ECC path gain factor.

$$H(T)=\begin{cases}1, & |V_{\rm ramp}|\le T,\\ 0, & |V_{\rm ramp}|>T,\end{cases}\quad (T>0),$$

where T is the threshold voltage, which is also the ramp reset voltage.

If $\Omega_{\rm IN}$ is a small constant value, and the ramp voltage satisfies $|V_{\rm ramp}|\le T$, then $H(T)=1$, a steady value obtained from Eq. (5) is shown as follow:

$$V_{\rm ramp}=\frac{\Omega_{\rm IN}K_0K_{\rm f1}}{K_{\rm c}},\quad (|V_{\rm ramp}|\le T). \tag{6}$$

Substituting Eq. (6) into Eq. (4) yields $\Omega_{\rm O}=0$, and DCL-FOG is in dead-zone at this time.

The dead-zone generation condition of DCL-FOG could be deduced from Eq. (6), and it is expressed as

$$|\Omega_{\rm IN}|\le\frac{K_{\rm c}T}{K_0K_{\rm f1}}. \tag{7}$$

When $\Omega_{\rm IN}$ is set to be a large constant. If the gyro is still out of dead-zone and the ramp voltage satisfies $|V_{\rm ramp}|=T$, then the ramp should be reset. Substituting the values of $|V_{\rm ramp}|=T$ and $V_{\rm ramp}=0$ into polynomial (4) yields the approximated steady output signals during ramp reset time and after the reset

time, respectively, as follows:

$$\Omega_{\rm o}^1 = \frac{\Omega_{\rm IN}K_0}{K_{\rm m}K_{\rm md}K_{\rm da}} \pm \frac{TK_{\rm c}}{K_{\rm m}K_{\rm md}K_{\rm da}K_{\rm f1}}, \quad (8)$$

$$\Omega_{\rm o}^0 = \frac{\Omega_{\rm IN}K_0}{K_{\rm m}K_{\rm md}K_{\rm da}}. \quad (9)$$

The output of gyro vibrated periodically is in a range $[\Omega_{\rm o}^0,\ \Omega_{\rm o}^1]$, and the vibration amplitude is $\left|\frac{TK_{\rm c}}{K_{\rm m}K_{\rm md}K_{\rm da}K_{\rm f1}}\right|$.

A simulation on FOG dead-zone and periodically vibration is launched based on the ECC model of DCL-FOG, which is shown in Fig. 6 and Eq. (4). The relevant parameters are listed in Table 3.

Table 3. Simulation parameters.

parameters	l/m	d/m	λ/μm	C/(m/s)	$K_{\rm f2}$	T/V	$K_{\rm md}$	$K_{\rm da}$/V	$K_{\rm m}$/(rad/V)	$K_{\rm f1}$	$K_{\rm c}$
values	300	0.04	1.3	3×10^8	10^6	4	100	$0.08/2^{16}$	1.57	0.02	10^{-2}

Set $\Omega_{\rm IN}$ to be a constant of 0.29 °/h, and the simulation results are shown in Fig. 7(a). The ramp voltage $V_{\rm ramp}$ rises with the accumulation of integration time, which leads to an augment of crosstalk-coupling in closed loop of FOG, and also causes a decrement of $\Omega_{\rm o}$. FOG will be in dead-zone in the case where $\Omega_{\rm o}$ decreases to 0 °/h before $V_{\rm ramp}$ achieves the threshold value T.

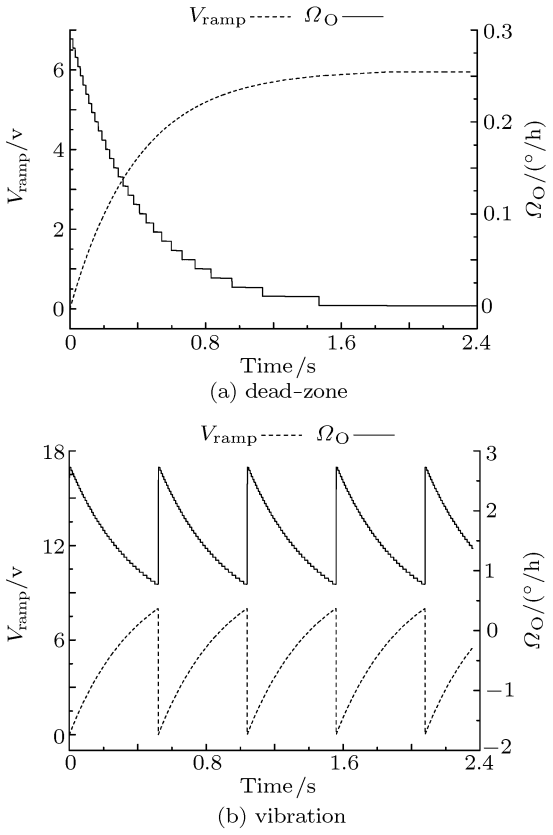


Fig. 7. Simulations of ramp voltage and output angular velocity for dead-zone (a) and vibration (b).

Set $\Omega_{\rm IN}$ to be a constant of 2.73 °/h, and the simulation results are shown in Fig. 7(b). With the accumulation of the integration time, the rising of $V_{\rm ramp}$ increases the crosstalk-coupling of FOG, and causes an offset of $\Omega_{\rm o}$ from the ideal value. The signal $V_{\rm ramp}$ is reset to be zero and $\Omega_{\rm o}$ is reset to be an ideal value if $V_{\rm ramp}$ achieves the threshold T before $\Omega_{\rm o}$ decreases to 0 °/h. A periodical vibration is generated when the above process is repeated.

The testing of dead-zone and periodic vibration was conducted on DCL-FOG, which included the modulation signal ECC, and for the testing method we referred to that in Refs. [12] and [13]. When the parameters of FOG in the setting are in Table 3, the testing results are shown in Fig. 8. The dead-zone of the tested FOG is 1.4 °/h; the bias stability, which includes the periodic vibration, is 0.72 °/h; the bias stability, which has filtered the periodic vibration off, is 0.28 °/h. Additionally, there appears an apparent nonlinearity of the gyro output, which is near the dead-zone.

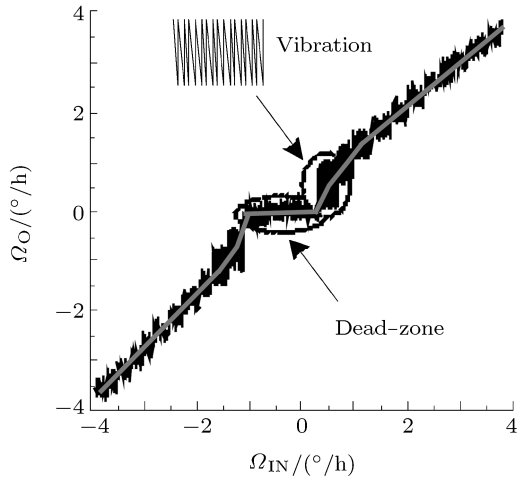


Fig. 8. Testing results of gyroscope dead-zone and periodic vibration.

From the analysis of Eq. (7), dead-zone is inversely proportional to parameters K_0 and K_{f1}. As described in Ref. [1], the accuracy of DCL-FOG is proportional to K_0 and K_{f1}. For the bias stability and the dead-zone test, the measurement results are listed in Table 4. Four fibre coils with the different settings were connected on to the tested FOG, and other parameters of optical and electronic components were kept fixed in the experiment. It can be observed that the dead-zone decreases with FOG accuracy increasing.

Table 4. Deadzone test results for different FOG accuracies.

l/m	d/m	bias stability/(°/h)	dead-zone/(°/h)
300	0.04	0.32	1.4
500	0.06	0.12	0.51
800	0.08	0.07	0.24
1000	0.1	0.5	0.14

There are two approaches to the attenuation of the ECC effect.

(i) An appropriate arrangement of electronic circuit position and a large printed circuit board area designed could segregate the modulation signal from the signal transmission channel, and further impair the ECC effect.

(ii) Random modulation could be utilised to eliminate the cross correlation between modulation signal and demodulation signal, which also conduces to ECC effect mitigation.[4,6]

However, none of these two approaches are excellent in practice. The first approach relies on the electronic circuit design and precision of manufacture, which makes quantitative analysis difficult. The second approach is hard to be utilised in high precision DCL-FOG, as it is affected by the linearity of modulator efficiency, and might bring an additional noise into FOG.[6]

4. Conclusion

The essential phase modulation and feedback controller might cause the ECC effect in DCL-FOG, which is discussed and verified in this paper. Several conclusions are summarised as follows:

(i) Four ECCs exist in the electronic structure of DCL-FOG, i.e. the ECC between the modulator driver and the source driver, the ECC between the modulator driver and the detector, the ECC between the modulator driver and the preamp and the ECC between the modulator driver and the A/D converter.

(ii) The open loop bias error that is generated by the ECC is a constant value if it is only a square wave modulation, and it would vary with the amplitude of ramp wave only when the modulation is a combination of the square wave and the ramp wave.

(iii) The difference in phase between demodulation signal and crosstalk signal varies with the amplitude of ramp, which leads to a variation of ECC generated open loop bias error.

(iv) The ECC of modulation signal might cause a dead-zone when a small angular velocity is inputted, and it might also lead to a periodic vibration of the bias error of gyro when a big angular velocity is inputed.

References

[1] Lefevre H C 1993 *The Fibre-Optic Gyroscope* (London: Artech House) p107–125

[2] Hotate K 1997 *Opt. Rev.* **4** 28

[3] Pavlath G A 1996 *Fibre Optic Gyros: 20th Anniversary Conference*, Denver, USA, August 5–6, 1996 p46

[4] Spahlinger G 1996 *Fibre Optic Gyros: 20th Anniversary Conference*, Denver, USA, August 5–6, 1996 p218

[5] Honthaas J, Buret T, Paturel Y and Gaiffe T 2006 *The 18th International Optical Fibre Sensors Conference*, Cancún, México, October 23–27, 2006 p69

[6] Jin J, Li M, Song N F and Zhang C X 2008 *J. Beijing Univ. Aeronaut. Astronaut.* **34** 769 (in Chinese)

[7] Gao J Z 2005 *Detection of Weak Signals* (Beijing: Tsinghua University Press) p242–245 (in Chinese)

[8] Noureldin A, Mintchev M, Halliday D I and Tabler H 1999 *Proceedings of the 1999 IEEE Canadian Conference on Electrical and Computer Engineering*, Edmonton, Alberta, Canada, May 9–12, 1999 p633

[9] Zhang C X, Tian H T, Li M, Jin J and Song N F 2008 *Chin. Phys.* B **17** 573

[10] Kincaid D and Cheney W 2002 *Numerical Analysis: Mathematics of Scientific Computing* (4rd ed) (USA: Brooks/Cole-Thomson Learning) p245–353

[11] Seidel C and Trommer G F 2004 *Electron. Lett.* **40** 166

[12] IEEE Std 528-2001 2001 *IEEE Standard for Inertial Sensor Terminology* (New York: The Institute of Electrical and Electronics Engineers, Inc) p36

[13] Song N F, Zhang C X and Jin J 2007 *Chin. Phys.* **16** 735